

Single Crystallization of an Inverse Bicontinuous Cubic Phase of a Lipid

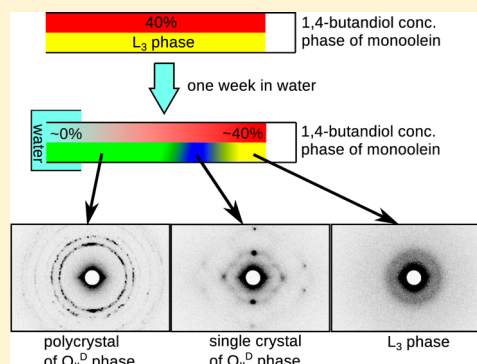
Toshihiko Oka^{*,†,§} and Hiroki Hojo[‡]

[†]Department of Physics, Graduate School of Science, [§]Nanomaterials Research Division, Research Institute of Electronics, and

[‡]Department of Physics, Faculty of Science, Shizuoka University, Shizuoka 422-8529, Japan

Supporting Information

ABSTRACT: We report a simple method to produce a single crystal region of an inverse bicontinuous cubic (Q_{II}) phase of a lipid, 1-monoolein. By starting with the lipid of the sponge (L_3) phase in the presence of 1,4-butanediol, we can obtain a single crystal region of the double-diamond Q_{II}^D phase in 1 week by controlled dilution of 1,4-butanediol. The length of the single crystal region in a 0.5 mm diameter capillary was on the order of millimeters. X-ray diffraction images of the region showed diffraction “spots”, but not “rings” as in powder diffraction. The diffraction images also changed rotation angle dependently. We could assign Miller indices to all of the distinguishable diffraction spots from the region. This method would bring benefits to the basic and applied research areas of the Q phases.



INTRODUCTION

Inverse bicontinuous cubic (Q_{II}) phases formed by biological amphiphiles, such as lipids, have attracted significant attention in terms of both their biological and physicochemical characteristics.^{1–3} The phases represent an interesting family that includes the double-diamond (Q_{II}^D), the primitive (Q_{II}^P), and the gyroid (Q_{II}^G) phases. This family of phases has 3D nanostructures composed of a curved fluid bilayer made from amphiphile molecules, which separates two interpenetrating continuous networks of water channels typically 2–5 nm in diameter.⁴ The Q_{II} phases are of great interest in various scientific fields. These phases are formed in biomembranes: prolamellar bodies of various plants,⁵ organized smooth endoplasmic reticulum,⁶ and the mitochondrial inner membrane in amoeba (*Chaos carolinensis*).⁷ There are a number of applications of the Q_{II} phase using its characteristic structure. This phase has been used as a matrix for the crystallization of membrane proteins,⁸ and the number of membrane proteins whose structure was solved with the phase are increased.⁹ In the pharmaceutical field, small particles of the Q_{II} phases, cubosomes, have been used as containers to deliver drugs.¹⁰

However, in many researches Q_{II} phase samples containing randomly oriented domains have been used thus far. In general, single-crystal materials have different properties compared to their polycrystal equivalents. Thus, it would be advantageous if there is a method to make a single-crystal domain of Q_{II} phases using biological amphiphiles. Pieranski's group has reported single crystallization methods for lyotropic systems, including 1-monoolein (MO), to research faceting of soft crystals.^{11,12} It might, however, be difficult for others to apply their methods because the methods typically include delicate control of the

temperature, humidity, and other factors using special apparatus.

In this paper, we show a simple method to make a single crystal region of the Q_{II}^D phase of a lipid, MO, from the sponge (L_3) phase. The L_3 phase can be considered to be a disordered Q_{II} phase that still displays a bicontinuous network of water channels separated by a lipid bilayer.¹³ It possesses short-range order, but it is disordered over longer length scales. This phase is visualized as a “melted” Q_{II} phase with a less curved lipid bilayer and two to three times larger aqueous pores than the Q_{II} phase.¹⁴ Amphiphiles that spontaneously form Q_{II} phases are often seen to form the L_3 phases in the presence of additives,¹⁵ e.g., 1,4-butanediol (BDO), 2-methyl-2,4-pentanediol. The additives relax the curvature of the Q_{II} phase, leading to a disordered structure of the L_3 phase.¹⁵ This phase is also used like the Q_{II} phase as a matrix for the crystallization of membrane proteins.¹⁶ To align the orientation of the Q_{II}^D phase, Seddon et al. used the L_3 – Q_{II}^D phase transition under shear.^{4,17} However, one can make only one dimensionally oriented sample by their method. We, therefore, developed a new method. We applied a counter-diffusion method used in protein crystallography to make a single crystal region of the Q_{II}^D phase of MO from the L_3 phase. By controlling the dilution speed of the BDO concentration, we could form a single crystal region of the Q_{II}^D phase. The single crystal region diffracts X-rays as spots, which are sufficient to determine the orientation of the crystallized region.

Received: May 22, 2014

Revised: June 29, 2014

Published: July 9, 2014

EXPERIMENTAL SECTION

A 60:40 v/v solution of water/BDO (Wako Pure Chemical Industries, Osaka, Japan) was prepared. The solution was mixed with dried MO (Sigma Chemical Co., St. Louis, MO, USA) in a 60:40 w/w solvent/MO ratio, and it underwent two freeze-thaw cycles.^{4,17} The L_3 phase sample was loaded into a polyimide capillary (PIT-S, Furukawa Electric Co., Tokyo, Japan), whose inner diameter was 0.5 mm and wall thickness was 0.04 or 0.06 mm. The length of the loaded sample was about 30 mm. One end of the sample was sealed with an adhesion bond of epoxy resin (Araldite RT30, Nichiban, Tokyo, Japan). The other end of the sample was soaked in 3 mL water at 25 °C (Figure 1). About 1 week later, X-ray diffraction measurements were carried out.

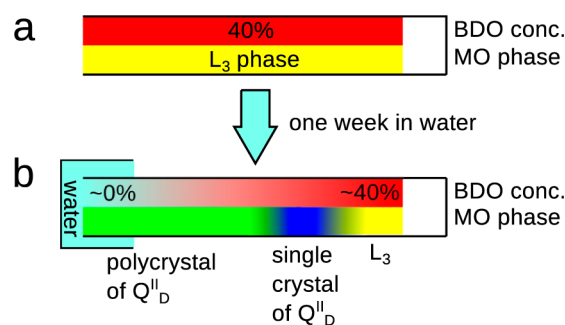


Figure 1. Schematic showing the process by which a single crystal region is formed in the capillary. To show BDO concentration and the MO phase, the capillary is colored as two separate stripes. (a) The MO sample before soaking in water. The sample in the capillary is homogeneous. The concentration of the BDO in the capillary is 40%, and the phase of the sample is L_3 . (b) Sample soaked in water for 1 week. A concentration gradient of the BDO is formed from end to end in the capillary. The lipid at the edge facing water forms a polycrystal of the Q_{II}^D phase. A single crystal region of the Q_{II}^D phase is formed between the L_3 phase and the polycrystal of the Q_{II}^D phase. The red tone indicates the concentration of BDO. Conditions of the MO sample are colored: the L_3 phase is yellow, the polycrystal region of the Q_{II}^D phase is green, and the single crystal region of the Q_{II}^D phase is blue. The capillaries were placed vertically in the actual experiment.

The X-ray diffraction measurements were performed in a laboratory small-angle X-ray scattering system (NANO-Viewer system, Rigaku, Tokyo, Japan). The rotating Cu anode generator was operated at 40 kV and 30 mA, thus the X-ray wavelength was 0.154 nm. X-ray diffraction patterns were measured using a two-dimensional detector (PILATUS 100K, Dectris, Baden, Switzerland). The sample-detector distance was set to about 510 mm, which was calibrated with silver behenate.¹⁸ The sample was mounted on a goniometer head 1005 (Huber, Rimsting, Germany), and the head was on a motorized rotation stage SGSP-60YAW-0B (Sigma Koki, Tokyo, Japan). The rotation axis was vertical. Measurement was performed at room temperature, which was kept at 25 °C. To search for a single crystal region, X-ray diffraction measurements were made by changing the position along the long axis of the sample capillary. We did not rotate the sample in this search. The lattice constants of the L_3 phase were calculated by assuming continuous disordering of the Q_{II}^D phase where the diffraction from the two groups of $\{1\ 1\ 0\}$ and $\{1\ 1\ 1\}$ planes broaden and merge into a single diffuse ring.¹⁵ To clarify whether a region was single crystal, we used the oscillation method to measure X-ray diffraction from the region. In this method, the sample was rotated in small oscillation angle steps during the X-ray exposures. For this experiment, X-ray diffraction was measured from 0° to 180° with oscillation steps of 10°. The number of oscillations in a single exposure was two, and the time of a single exposure was 60 sec.

The crystallographic space group of the Q_{II}^D phase is $Pn\bar{3}m$ and the crystal system is cubic. To decide the orientation of the single crystal region from X-ray diffraction images of the oscillation method, we used a set of diffraction spots from the set of $\{2\ 0\ 0\}$ planes as a

standard of the crystal orientation. The set includes six planes, $(2\ 0\ 0)$, $(\bar{2}\ 0\ 0)$, $(0\ 2\ 0)$, $(0\ \bar{2}\ 0)$, $(0\ 0\ 2)$ and $(0\ 0\ \bar{2})$. To define the orientation of the single crystal, we used Euler angles¹⁹ with axis rotation sequence of Z-X-Z, and rotation angles α, β, γ . Using the calculated Euler angles, we indexed the diffraction spots of the images. Finally, we optimized the Euler angles and lattice constant by using all of the assigned spot positions. The intensity was calculated by integrating the spot areas and subtracting background intensities of same size areas. The image processing and analysis software ImageJ²⁰ was used to locate peak spots and perform intensity integrations.

RESULTS AND DISCUSSION

Figure 2 shows X-ray diffraction images obtained from the capillary sample after 1 week of soaking in water at various

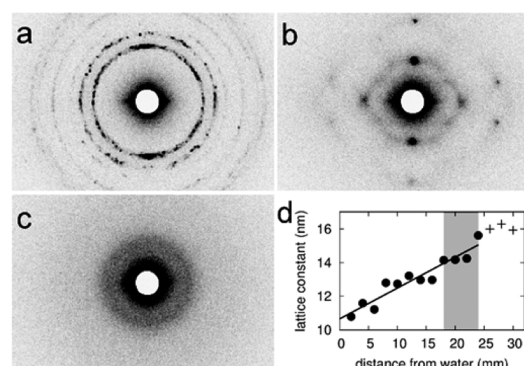


Figure 2. X-ray diffraction images of the MO sample after 1 week of soaking in water without oscillation. (a) At 2 mm from the edge facing bulk water. Diffraction from the polycrystal of the Q_{II}^D phase. (b) At 22 mm. Diffraction from the single crystal region. (c) At 28 mm. Diffraction from the L_3 phase. (d) Relation between distance from water and lattice constants of phases calculated from X-ray diffraction patterns. The Q_{II}^D phases are shown as filled circles; the L_3 phases are shown as crosses. The shaded region is the single crystal region estimated from the X-ray diffraction pattern.

distances from the bulk water. Figure 2a shows data obtained at a distance of 2 mm, which is one end of the sample near the bulk water. Indexing of the peaks indicates the phase of this region to be the Q_{II}^D phase (Supporting Information Figure S1). Randomly oriented small crystalline regions diffract X-rays concentrically. We can distinguish many spots on the concentric diffraction rings, with each spot coming from a small single crystal in the polycrystal material. Figure 2c shows the scattering at 28 mm from the water, which is near the other end of the sample. The image shows a diffuse diffraction ring, and the phase is considered to be the L_3 phase.^{4,15} Figure 2b shows the scattering at 22 mm. This diffraction pattern shows several spots with vertical and horizontal symmetry. This diffraction pattern is completely different from the powder pattern shown in Figure 2a, indicating that the sample at 22 mm might be single crystal region of a phase. Sequential diffraction images from the capillary sample from 2 mm to 30 mm distances are given in the Supporting Information (Figure S2). The images clearly demonstrate position-dependent change. From 2 mm to 16 mm, the number of diffraction spots on concentric rings decreased as the distance from the water increased. The images from 18 mm to 24 mm have diffraction spots at almost the same positions, which indicates that these regions might be single crystal and seem to spread from 18 mm to 24 mm. The images from 24 mm to 30 mm show a broad diffraction peak with central symmetry, which

indicates that the phase of this region is the L_3 phase. Thus, the region might be single crystal is located between the L_3 phase and the polycrystal region of the Q_{II}^D phase. Figure 2d shows that the lattice constants depend linearly on distance from water.

To study the sample region around 22 mm from the bulk water, we used the oscillation method to measure X-ray diffraction. As the sample rotates, X-ray diffraction changes angle dependently (Figure 3, Supporting Information Figure

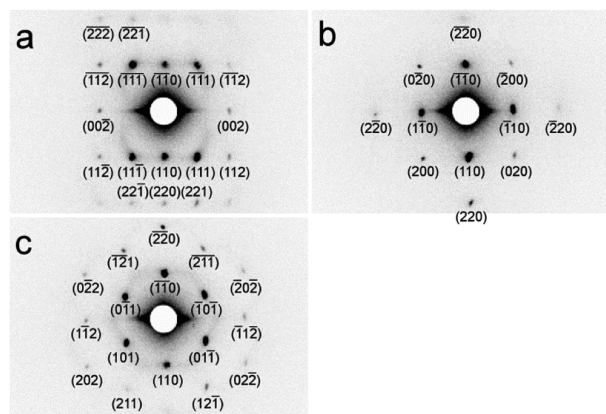


Figure 3. X-ray diffraction images of the MO sample at 22 mm with an oscillation angle of 10° . (a) At 10° . (b) At 100° . (c) At 150° . The assigned Miller indices are also shown.

S3). Diffraction spots in the images are apart from the adjacent ones, and look like grid points. We, therefore, considered the region to be single crystal. Next we assigned Miller indices to all distinguishable diffraction spots up to a set of $\{2\ 2\ 2\}$ planes. Part of the assigned indices is shown in Figure 3. We can see the diffraction spots from $(1\ 1\ 0)$ and $(\bar{1}\ \bar{1}\ 0)$ planes in all the images of Figure 3, which indicates that the $[1\ 1\ 0]$ direction of the single crystal region is almost parallel to the rotation axis and the long axis of this capillary sample. The space group of the Q_{II}^D phase is $Pn\bar{3}m$, and the extinction rule of $Pn\bar{3}m$ indicates that diffraction spots from the set of $\{1\ 0\ 0\}$ and $\{2\ 1\ 0\}$ planes are unobservable. Actually, we could not distinguish these diffraction spots in all the images. The lattice constant of this Q_{II}^D single crystal region is refined to be 14.7 nm. This value is almost the same as that observed at the transition point from Q_{II}^D to the L_3 phase in the presence of BDO.¹⁵ The refined Euler angles, α, β, γ , are $78^\circ, 90^\circ, 47^\circ$, respectively. The integrated and averaged intensities of distinguishable diffraction spots were shown in Supporting Information (Table S1). The intensities decreased rapidly at higher diffraction angle (where the Miller indices increased). The decreasing rate of the intensities is fairly larger than that of the model calculation.²¹ Deducing from the lattice constant of the single crystal region, the solution in the water channel contained about 25% of BDO.¹⁵ Thus, the lipid bilayer of the region does not seem well-oriented. On the other hand, X-ray diffraction experiments showed that only a single crystal region exists in the exposure area. Moreover, the single crystal region was spread from 18 mm to 24 mm in the 0.5 mm diameter capillary (Supporting Information Figure S2). The volume of the single crystal region is therefore considered to be of the $\sim\text{mm}^3$ order. Similar situations frequently occur in the crystallization of proteins. Some protein crystals with sharp edges diffract X-rays weakly, and one can observe few spots around the beam stop.²²

A counter-diffusion method is used in protein crystallography to optimize crystallization conditions. In one variation of the counter-diffusion method, precipitant solutions are placed on a gel containing the protein solution.²³ Diffusion of the precipitant solution into and through the gel regulates the delivery of precipitant to the protein solution and forms a precipitant concentration gradient from end to end in the capillary. We applied the counter-diffusion method to make a single crystal region of a Q_{II} phase (Figure 1). In our method, the gel was replaced by the Q_{II} phase itself, which is considered to retard diffusion of BDO and water. The relationship between lattice constants and the distance from the sample edge facing the bulk water are shown in Figure 2d. The lattice constants of the Q_{II}^D phases are nearly proportional to the distance from the bulk water. Cherezov et al.¹⁵ showed that the lattice constants of the Q_{II}^D phases are proportional to the concentration of BDO. The concentration of BDO in our sample, therefore, would almost be proportional to the distance from the bulk water. The estimated BDO concentration in the single crystal region is about 25%. The lattice constant of the L_3 phase before soaking in water was 16.8 nm. Considering from the lattice constant of the L_3 phase in Figure 2d, the concentration of BDO at 30 mm would slightly decrease from the initial value of 40%. BDO concentration at which the L_3 – Q_{II}^D phase transition occurs is considered to be adequate for crystal growth. A region of the concentration, which is located at the edge of the Q_{II}^D phase, moves from the edge facing bulk water to the other end as dilution of BDO advances. Thus, freshly formed Q_{II}^D phase always adjoins the region adequate for crystal growth, and next Q_{II}^D phase is formed in the region. Speed of the movement of the region is fast near the edge-facing bulk water, while slow at the other end. The region of single crystal, therefore, would grow large at distant region from the water. Actually, polycrystals of the Q_{II}^D phase was formed at the edge region facing water, while single crystal was formed at the distant region.

To check the reproducibility of this experiment, we repeated same experiments several times. In every experiments, we obtained single crystal regions. Quality of the single crystal regions, however, was not always same; spots split and/or broadened in some samples. In the present experiment, the $[110]$ direction of the single crystal region was parallel to the long axis of the sample capillary. However, diffraction data from the other samples did not show this orientation. Thus, we consider that the orientation of the single crystal region depends on that of the crystal nucleus. Single crystal regions started to form about two or 3 days after water soaking. However, the single crystal regions diffract X-rays better after about 1 week. An appropriate BDO concentration for single crystallization would be formed and kept at around 1 week. Qualities of the regions deteriorated after about 2 weeks, probably because a decrease in BDO concentration causes a decrease in the lattice constant of the region.

Pieranski's group has reported single crystallization of lyotropic systems, including MO, while investigating faceting of soft crystals.^{11,12} They used the inverted micellar phases (L_2) of MO to transform a single crystal of the Q_{II}^G phase by changing the relative humidity and temperature, and they observed the single crystallization at the L_2/Q_{II}^G interface. We observed single crystallization at the interface where the phase transition occurred from the L_3 to the Q_{II}^D phase. The L_2 and L_3 phases are isotropic and are liquids with high fluidity. In contrast, the Q_{II}^G and Q_{II}^D phases are nonisotropic and stiff

liquid crystals. Thus, a high fluidity liquid phase such as L_2 and L_3 would be required for single crystal growth of the Q_{II} phases. In the phase diagram of the MO/water system,²⁴ the Q_{II}^G phase adjoins the L_2 phase, while the Q_{II}^D phase has no adjacent liquid phase. It might therefore be difficult to form a single crystal region of the Q_{II}^D phase without additives, which transform the MO/water system into the L_2 or L_3 phase. We used BDO to make a single crystal region of the Q_{II}^D phase of MO. Cherezov et al.¹⁵ reported that the Q_{II}^D phase of MO could be converted to the L_3 phase by increasing the concentration of additives, including BDO. Other additives might be alternatives to form single crystals.

One of the candidates to which the single-crystallization method could be applied is a study of the mechanism involved in the phase transitions between the bilayer liquid-crystalline (L_a) phase and the Q_{II} phases, and also between the different Q_{II} phases. Elucidation of this mechanism would contribute to an understanding of topological transformation of biological membranes, including membrane fusion. The X-ray powder diffraction technique has been widely used in structural analysis of the Q_{II} phase to determine the phase of amphiphiles,^{15,25} for time-resolved phase transition studies,²⁶ and to reconstruct the electron density of the Q_{II} phase.^{27,28} However, the data from this technique does not contain information on sample orientation. Recently, preparation methods of films to align one axis of the Q_{II}^D phase have been reported^{4,17,29} and applied to research the epitaxial relation in phase transition.^{29,30} These alignment techniques, including our method, promise to yield high quality structural information for the Q_{II} phases.

OUTLOOK

We have demonstrated a simple method to produce a single crystal region of the Q_{II}^D phase of a lipid at room temperature. This has been achieved by controlled dilution of BDO, and the single-crystal region was observed near the concentration where phase transition occurred from the L_3 to the Q_{II}^D . X-ray diffraction images showed clear diffraction spots, which indicated the quality of the single crystal region was good. This method would bring benefits to the basic and applied research areas of the Q_{II} phases.

ASSOCIATED CONTENT

Supporting Information

A circular averaged profile of Figure 2a, sequential X-ray diffraction images for Figure 2a–c and Figure 3, and a table of averaged intensities of diffractions. This material is available free of charge via the Internet at <http://pubs.acs.org>.

AUTHOR INFORMATION

Corresponding Author

*E-mail: stoka@ipc.shizuoka.ac.jp.

Notes

The authors declare no competing financial interest.

ACKNOWLEDGMENTS

X-ray diffraction experiments were carried out at the Center for Instrumental Analysis of Shizuoka University. We are grateful for Prof. M. Yamazaki for helpful discussions and critical reading of the manuscript. Preliminary results were obtained at the BL40B2 beamline of SPring-8 (Hyogo, Japan), under the approval of the Japan Synchrotron Radiation Research Institute (JASRI) (Proposal No. 2013B1270).

REFERENCES

- (1) Seddon, J. M.; Templer, R. H. Polymorphism of Lipid–Water Systems. In *Structure and Dynamics of Membranes*; North-Holland: Amsterdam, 1995; Vol. 1, Chapter 3, pp 97–160.
- (2) Almsherg, Z. A. Cubic Membranes: A Legend beyond the Flatland* of Cell Membrane Organization. *J. Cell Biol.* **2006**, *173*, 839–844.
- (3) Yamazaki, M. Transformation Between Liposomes and Cubic Phases of Biological Lipid Membranes Induced by Modulation of Electrostatic Interactions. In *Advances in Planar Lipid Bilayers and Liposomes*; Academic Press: Oxford, U.K., 2009; Vol. 9, Chapter 7, pp 163–209.
- (4) Seddon, A. M.; Lotze, G.; Plivelic, T. S.; Squires, A. M. A Highly Oriented Cubic Phase Formed by Lipids under Shear. *J. Am. Chem. Soc.* **2011**, *133*, 13860–13863.
- (5) Murakami, S.; Yamada, N.; Nagano, M.; Osumi, M. Three-Dimensional Structure of the Prolamellar Body in Squash Etioplasts. *Protoplasma* **1985**, *128*, 147–156.
- (6) Landh, T. From Entangled Membranes to Eclectic Morphologies: Cubic Membranes as Subcellular Space Organizers. *FEBS Lett.* **1995**, *369*, 13–17.
- (7) Deng, Y.; Mieczkowski, M. Three-Dimensional Periodic Cubic Membrane Structure in the Mitochondria of Amoebae *Chaos carolinensis*. *Protoplasma* **1998**, *203*, 16–25.
- (8) Cherezov, V.; Caffrey, M. Membrane Protein Crystallization in Lipidic Mesophases. A Mechanism Study Using X-ray Microdiffraction. *Faraday Discuss.* **2007**, *136*, 195.
- (9) Cherezov, V. Lipidic Cubic Phase Technologies for Membrane Protein Structural Studies. *Curr. Opin. Struct. Biol.* **2011**, *21*, 559–566.
- (10) Drummond, C. J.; Fong, C. Surfactant Self-Assembly Objects as Novel Drug Delivery Vehicles. *Curr. Opin. Colloid Interface Sci.* **1999**, *4*, 449–456.
- (11) Leroy, S.; Grenier, J.; Rohe, D.; Even, C.; Pieranski, P. Anisotropic Surface Melting in Lyotropic Cubic Crystals. *Eur. Phys. J. E* **2006**, *20*, 19–27.
- (12) Pieranski, P. Chapter One - Faceting of Soft Crystals. In *Advances in Planar Lipid Bilayers and Liposomes*; Aleš Iglič, Ed.; Academic Press, 2011; Vol. 14, pp 1–43.
- (13) Porte, G. Isotropic Phases of Bilayers. *Curr. Opin. Colloid Interface Sci.* **1996**, *1*, 345–349.
- (14) Ridell, A.; Ekelund, K.; Evertsson, H.; Engström, S. On the Water Content of the Solvent/Monoolein/Water Sponge (L_3) Phase. *Colloids Surf. Physicochem. Eng. Asp.* **2003**, *228*, 17–24.
- (15) Cherezov, V.; Clogston, J.; Papiz, M. Z.; Caffrey, M. Room to Move: Crystallizing Membrane Proteins in Swollen Lipidic Mesophases. *J. Mol. Biol.* **2006**, *357*, 1605–1618.
- (16) Wadsten, P.; Wöhri, A. B.; Snijder, A.; Katona, G.; Gardiner, A. T.; Cogdell, R. J.; Neutze, R.; Engström, S. Lipidic Sponge Phase Crystallization of Membrane Proteins. *J. Mol. Biol.* **2006**, *364*, 44–53.
- (17) Squires, A. M.; Hallett, J. E.; Beddoes, C. M.; Plivelic, T. S.; Seddon, A. M. Preparation of Films of a Highly Aligned Lipid Cubic Phase. *Langmuir* **2013**, *29*, 1726–1731.
- (18) Huang, T. C.; Toraya, H.; Blanton, T. N.; Wu, Y. X-ray Powder Diffraction Analysis of Silver Behenate, a Possible Low-Angle Diffraction Standard. *J. Appl. Crystallogr.* **1993**, *26*, 180–184.
- (19) Goldstein, H. *Classical Mechanics*; Addison-Wesley Pub. Co.: Reading, MA, 1980.
- (20) Schneider, C. A.; Rasband, W. S.; Eliceiri, K. W. NIH Image to ImageJ: 25 Years of Image Analysis. *Nat. Methods* **2012**, *9*, 671–675.
- (21) Harper, P. E.; Gruner, S. M. Electron Density Modeling and Reconstruction of Infinite Periodic Minimal Surfaces (IPMS) Based Phases in Lipid-Water Systems. I. Modeling IPMS-Based Phases. *Eur. Phys. J. E: Soft Matter Biol. Phys.* **2000**, *2*, 217–228.
- (22) Heras, B.; Edeling, M. A.; Byriel, K. A.; Jones, A.; Raina, S.; Martin, J. L. Dehydration Converts DsbG Crystal Diffraction from Low to High Resolution. *Structure* **2003**, *11*, 139–145.
- (23) Garcia-Ruiz, J. M.; Gonzalez-Ramirez, L. A.; Gavira, J. A.; Otálora, F. Granada Crystallisation Box: A New Device for Protein

Crystallisation by Counter-Diffusion Techniques. *Acta Crystallogr. D: Biol. Crystallogr.* **2002**, *58*, 1638–1642.

(24) Qiu, H.; Caffrey, M. The Phase Diagram of the Monoolein/Water System: Metastability and Equilibrium Aspects. *Biomaterials* **2000**, *21*, 223–234.

(25) Okamoto, Y.; Masum, S. M.; Miyazawa, H.; Yamazaki, M. Low-pH-Induced Transformation of Bilayer Membrane into Bicontinuous Cubic Phase in Dioleoylphosphatidylserine/Monoolein Membranes. *Langmuir* **2008**, *24*, 3400–3406.

(26) Alam, M. M.; Oka, T.; Ohta, N.; Yamazaki, M. Kinetics of Low pH-Induced Lamellar to Bicontinuous Cubic Phase Transition in Dioleoylphosphatidylserine/monoolein. *J. Chem. Phys.* **2011**, *134*, 145102.

(27) Luzzati, V.; Mariani, P.; Delacroix, H. X-ray Crystallography at Macromolecular Resolution: A Solution of the Phase Problem. *Makromol. Chem. Macromol. Symp.* **1988**, *15*, 1–17.

(28) Harper, P. E.; Gruner, S. M.; Lewis, R. N. A. H.; McElhaney, R. N. Electron Density Modeling and Reconstruction of Infinite Periodic Minimal Surfaces (IPMS) Based Phases in Lipid–Water Systems. II. Reconstruction of D Surface Based Phases. *Eur. Phys. J. E: Soft Matter Biol. Phys.* **2000**, *2*, 229–245.

(29) Rittman, M.; Amenitsch, H.; Rappolt, M.; Sartori, B.; O'Driscoll, B. M. D.; Squires, A. M. Control and Analysis of Oriented Thin Films of Lipid Inverse Bicontinuous Cubic Phases Using Grazing Incidence Small-Angle X-Ray Scattering. *Langmuir* **2013**, *29*, 9874–9880.

(30) Seddon, A. M.; Hallett, J.; Beddoes, C.; Plivelic, T. S.; Squires, A. M. Experimental Confirmation of Transformation Pathways between Inverse Double Diamond and Gyroid Cubic Phases. *Langmuir* **2014**, *30*, 5705–5710.